Dear editor,

We would like to thank the referees for their reports, and we are pleased to see that they are overall positive about our manuscript. The questions in the report mainly deal with the computational efficiency of the method, its possible extensions, and the details of the structure factor. We have improved our manuscript to clarify these points. Below, we discuss the points made in the report and the requested changes one by one. With these changes, listed at the end of this document, we believe our manuscript is suitable for publication in SciPost Physics.

Yours sincerely,

The authors

Report

"In this work, Schobert et al performed an interesting study on CDW systems for exploring anharmonic potential energy surfaces accurately and efficiently using downfolded models to DFT and ab initio MD. They studied three different downfolding strategies and considered four different systems (1H-TaS_2, 1T-$TiSe_2$, 1H-NbS_2, and a carbon chain) to find that the models are very beneficial reducing by a large factor the complexity of ab initio MD electronic structure calculations. The work is very interesting and deserves publication as it indeed offers a route for speeding up path integral simulations of quantum nuclear effects which are rather cumbersome to be applied for extended systems."

We thank the referee for their positive assessment of our work.

Requested changes

1. Typo

"Typo p.12: "for the case example of monolayer"."

We thank the referee for noticing the typo, and we corrected it accordingly.

2. Expensive DFT calculations: Quantify supercell size

"p.4 : "since DFT calculations with large supercells are prohibitively expensive" Maybe the authors could quantify further the supercell size and explain why is needed in more detail."

Our simulation of the structure factor in Fig. 9 involves an 18×18 supercell which contains 10^3 atoms. In Fig. 7, we show results up to a 40×40 supercell ($5 \cdot 10^3$ atoms). On the other hand, in that benchmark, we were able to do direct DFT calculations only up to approximately 9×9 supercells ($3 \cdot 10^2$ atoms). This difference in scale is substantial, especially when one is interested in the regime close to a phase transition, where long-ranged correlations are important. We have inserted a forward reference into the text on page 4 to clarify this point.

Generally speaking, simulations involving smaller systems often give rise to finite size effects that can significantly influence the results. To illustrate these effects, we present the heat capacity from classical MD simulations conducted on supercell sizes ranging from 6×6 to 21×21 (see Fig. 1 of this reply).

Upon observation, it becomes evident that despite achieving convergence in terms of simulation steps, the curves exhibit a noticeable shift towards higher temperatures (higher T_{CL}) solely due to the variation in system size. Moreover, the shape of the peak becomes more pronounced with increasing system dimensions. While there is only a rather broad peak in C_V in the 6×6 case, that peak markedly increases for the larger supercells and develops towards a shape reminiscent of a jump discontinuity – indicative of a second-order phase transition – for the 21×21 system.

Therefore, finite size effects can induce not only quantitative alterations in simulation data but also qualitative changes.

3. Comparison of computational efficiency between all models

"Can the authors comment in more detail on the relative comparison of the models with respect to computational efficiency?"

Also here we thank the referee for the remark to give information on the computational power of all three models. Indeed we only stated the computational efficiency of the downfolded model III vs. DFT. As this model is non-interacting, it is the fastest of all three models. Model I and II require self-consistency cycles in the Hartree algorithm. Assuming a typical number of ~ 10 cycles needed for convergence, the speedup should be on the order of 10^4 rather than 10^5 for the example discussed with model I. We included a corresponding statement in the manuscript.

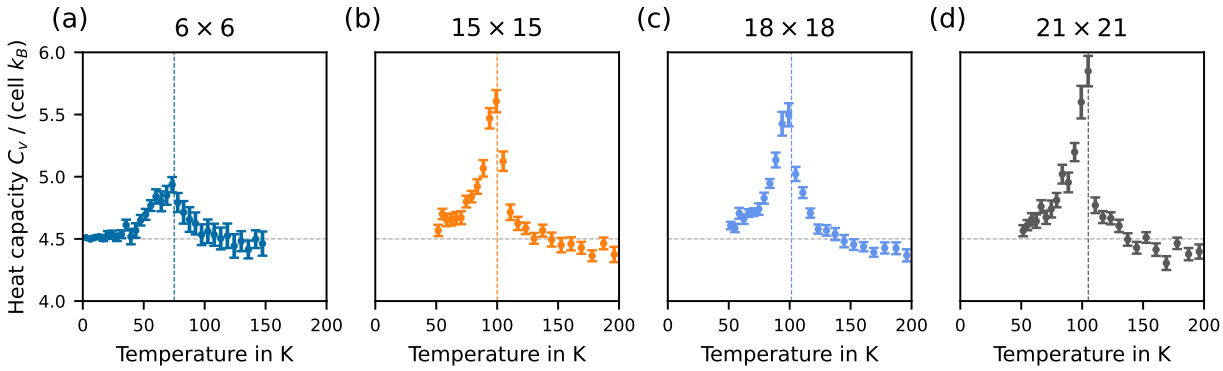

Figure 1: Heat capacity of monolayer 1H TaS_2 obtained with classical MD simulations.

4. Questions related to the structure factor (Eq. 19)

(a-1) *"Are the atomic scattering amplitudes missing from the equation of the structure factor?"*

The referee is correct; the atomic scattering amplitudes are not included in the formula presented in our manuscript. This omission is intentional, as our focus is solely on the movement of the tantalum atoms. In the following, we address this question by deriving Eq. (19) from the manuscript:

The scattering amplitude is defined by (cf. Eq. (2.4) of Ref. [1])

$$\Psi(\boldsymbol{q}) = \frac{1}{\langle f \rangle} \sum_{\nu} f_\nu e^{-i\boldsymbol{q}\cdot\boldsymbol{R}_\nu}, \tag{1}$$

where f_ν are the atomic scattering amplitudes. The intensity is given by the absolute square of the amplitude

$$I(\boldsymbol{q}) = |\Psi(\boldsymbol{q})|^2 = \frac{1}{\langle f \rangle^2} \sum_{\nu\mu} f_\nu f_\mu e^{-i\boldsymbol{q}\cdot\boldsymbol{R}_\nu} e^{i\boldsymbol{q}\cdot\boldsymbol{R}_\mu}. \tag{2}$$

As it is known that the displacements of the tantalum atoms are most significant within the CDW, we evaluate the intensity for this atomic species only. Thus, for identical atoms, the formula reduces to

$$I(\boldsymbol{q}) = \sum_{\nu\mu} e^{i\boldsymbol{q}\cdot(\boldsymbol{R}_\mu - \boldsymbol{R}_\nu)}. \tag{3}$$

Normalizing the expression leads to the *static structure factor* [2, 3]

$$S(\boldsymbol{q}) = \frac{I(\boldsymbol{q})}{N_{\mathrm{at}}^2} = \frac{1}{N_{\mathrm{at}}^2} \sum_{\nu\mu} e^{i\boldsymbol{q}\cdot(\boldsymbol{R}_\mu - \boldsymbol{R}_\nu)} = \frac{1}{N_{\mathrm{at}}^2} \left| \sum_{\nu=1}^{N_{\mathrm{at}}} e^{-i\boldsymbol{q}\cdot\boldsymbol{R}_\nu} \right|^2. \tag{4}$$

Thus, the formula for the structure factor has been streamlined to its minimal version, which is essentially a simple Fourier transform of the atomic positions.

(a-2) *"How is this relation related to diffuse scattering?"*

The formula Eq. (4) includes Bragg and all orders of thermal diffuse scattering contributions. The atomic positions can be written as deviations from the average lattice positions: $\boldsymbol{R}_\nu = \langle \boldsymbol{R}_\nu \rangle + \boldsymbol{u}_\nu$. The Bragg contribution is determined with respect to the average positions only (cf. Eq. (2.22) of Ref. [1]),

$$S_{\mathrm{BG}}(\boldsymbol{q}) = \frac{1}{N_{\mathrm{at}}^2} \left| \sum_{\nu=1}^{N_{\mathrm{at}}} e^{-i\boldsymbol{q}\cdot\langle \boldsymbol{R}_\nu \rangle} \right|^2. \tag{5}$$

Consequently, the diffuse scattering intensity is given by $S_{\mathrm{D}}(\boldsymbol{q}) = S(\boldsymbol{q}) - S_{\mathrm{BG}}(\boldsymbol{q})$. It is crucial to carefully define the average atomic positions, which should be considered in the static limit concerning the real-time propagation of a trajectory: $\langle R_\nu \rangle = \lim_{t\to\infty} \langle R_\nu(t) \rangle$. While replica-exchange MD simulations efficiently sample the phase space, it is important to note that they do not represent a real-time propagation of MD trajectories. Frequent replica exchanges can result in ambiguities regarding average positions, particularly affecting the Bragg signal.

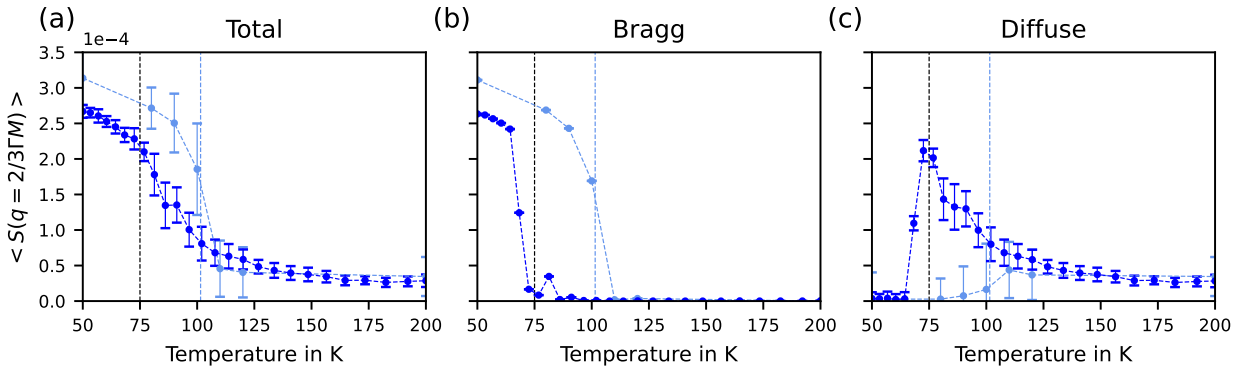

Figure 2: Separation of the total structure factor into Bragg and diffuse scattering contributions. The classical curves (light blue) originate from single NVT simulations at different temperatures, whereas the quantum mechanical curves (blue) result from the replica-exchange PIMD simulations.

In Fig. 2, we depict the Bragg signal obtained from replica-exchange PIMD simulations within a time interval where only a few replica-exchange events have occurred. The corresponding average lattice positions characterize the CDW in the low-temperature scenario, leading to a pronounced Bragg signal. As the system undergoes a phase transition, the Bragg signal vanishes, and the total structure factor becomes dominated by diffuse scattering contributions.

In the case of classical REMD, our data did not provide a sufficiently extended interval with only a few replica exchanges. Instead, we illustrate the same separation by employing individual canonical ensemble (NVT) simulations at specific temperatures. NVT simulations are known for conducting real-time propagations, resulting in well-defined average lattice positions. The light blue curves in Fig. 2 exhibit a qualitatively similar behavior to the quantum mechanical case. Yet, the separation of Bragg and diffusive contributions requires a very careful convergence analysis and will require additional simulations, which are in principle possible but beyond the scope of the present work.

(b) *"How many scattering wavevectors are used for the sampling? To me it looks to be a coarse grid."*

We have access to a grid of $18 \times 18 = 324$ scattering wavevectors $\boldsymbol{q}$, which are commensurate with the chosen supercell.

(c) *"How many configurations are needed to obtain a converged average?"*

We simulated both classical and path integral MD for at least 400 picoseconds. With a time step of 4 femtoseconds and printing every 20th step only, we end up with at least 5000 different configurations. As can be seen in Fig. 9, this leads to small error bars overall.

(d) *"What is the nature of CDW peaks? Is it quasi-elastic or inelastic?"*

In our manuscript, we evaluate the static structure factor, which is the frequency integrated version of the dynamic structure factor (cf. Eq. (4) of Ref. [4])

$$S(\boldsymbol{q}) = \hbar \int_{-\infty}^{+\infty} S(\boldsymbol{q}, \omega) d\omega. \tag{6}$$

For elastic scattering, one would need to evaluate the dynamic structure factor at $S(\boldsymbol{q}, \omega = 0)$, which is not the same as $S(\boldsymbol{q})$. Thus, in order to distinguish between quasi-elastic and inelastic peaks, one would need the dynamic structure factor.

Extracting the dynamic structure factor would require additional simulations in the NVT ensemble for the classical MD part. While the speed-up gained from downfolding facilitates such calculations, we leave the simulations of the dynamic structure factor (including all convergence checks) for future work.

(e) *"Can the authors comment whether this term includes contributions to diffuse scattering both from coupled and independent lattice vibrations (one-phonon and multiphonon scattering)?"*

Looking again at the scattering amplitude, we can expand the exponential factor of the displacements (cf. Eq. (2.20) of Ref. [1])

$$\Psi(\boldsymbol{q}) = \frac{1}{\langle f \rangle} \sum_{\nu} f_{\nu} e^{-i\boldsymbol{q}\cdot\boldsymbol{R}_{\nu}} = \frac{1}{\langle f \rangle} \sum_{\nu} f_{\nu} e^{-i\boldsymbol{q}\cdot\boldsymbol{R}^{0}_{\nu}} [1 + i\boldsymbol{q}\cdot\boldsymbol{u}_{\nu} + \dots], \tag{7}$$

where the first term of the expansion (1) corresponds to the Bragg signal, the second term ($i\boldsymbol{q}\cdot\boldsymbol{u}_{\nu}$) to first-order diffuse scattering and the higher order terms ($\dots$) belong to higher-order diffuse scattering. Since we are not truncating the displacements in any way, we have access to all orders of diffuse scattering.

5. Double definition of N

"Is there a double definition of N? Does it represent the number of k-points and number of atoms? I think it's better for the authors to make sure that no definitions with the same symbol appear in the text."

The referee is right and we agree that there should not be two definitions of the same symbol. We changed the definition of the number of atoms in the revised manuscript.

6. Cite newest EPW paper

"Let me also suggest a new paper for the EPW code: https://doi.org/10.1038/s41524-023-01107-3"

We thank the referee for pointing us to the latest EPW paper and cited it in the manuscript accordingly.

7. Improve models II and III by using anharmonic force constants and non-perturbative electron-phonon couplings

"Can the authors comment if anharmonic temperature-dependent lattice constants C^{DFT} can be used in Models II and III? Will it be more appropriate? More, will it be more beneficial and more consistent if the deformation potential is computed with nonperturbative supercell calculations to electron-phonon coupling (see for example: https://doi.org/10.1088/1367-2630/aaf53f)? I am simply sharing thoughts here."

The generic form of the downfolded model does contain anharmonic terms in the nuclear Hamiltonian, Eq. (6), and also higher order couplings, Eq. (7), which one could indeed attempt to derive from non-perturbative supercell calculations as the reviewer suggests. Inclusion of these kinds of higher-order terms to the downfolded models (with appropriate unscreening) would indeed be a promising direction to be worth exploring in future research. It might facilitate the downfolding approach to enter a regime of larger much distortions than based on the approximations involved in Eq. (8) and Eq. (9).

A corresponding remark has been added to the concluding section of our paper.

8. Data availability

"Will the first-principles calculations (inputs and outputs) uploaded to a database or the Python codes on open-source platforms?"

We welcome the trend toward increasing open-source data availability and express our gratitude for this recommendation. The Python codes are incorporated within the open-source software package `elphmod`, which we have cited in the manuscript and is available on GitHub. We have made all data and further source code available on Zenodo and added a corresponding Data Availability Statement.

9. Expand the work with temperature dependent electronic structure

"I think the work has some more space to be expanded for example in the calculation of other thermal averages related to the electronic structure."

We agree with the reviewer that our work opens several directions for extensions towards the study of additional phenomena and observables. These include the "thermal averages of the electronic properties" like the effective band structure in the presence of moving atoms but also the extraction of dynamic correlation functions involving the nuclear degrees of freedom. Since the purpose of this study was to introduce and benchmark the method of downfolded lattice models, we prefer to outline the aforementioned directions for extension and future directions as outlook in the concluding section of our paper.

List of changes

- *Change in Funding information:* AS and TW further acknowledge funding and support from the European Commission via the Graphene Flagship Core Project 3 (grant agreement ID: 881603).

- *Change in Sec. 2.1.2:* In the following, we will explain and demonstrate the downfolding according to models I–III along the ~~case~~ example case of monolayer 1H-TaS_2.
- *Change in Sec. 4:* As a demonstration of this enhancement, we perform the downfolding-based MD for the ~~case~~ example case of monolayer 1H-TaS_2 in Section 4.2.
- *Change in Sec. 2:* However, ~~since~~ DFT calculations with large supercells ~~are~~ can become prohibitively expensive (cf. Fig. 7 for benchmark calculations later in this work). As a consequence, DFT simulations of phase transitions governed by inhomogeneity effects are often very challenging. It is, thus, desirable to obtain energies and forces in a cheaper way, while remaining close to the quantum mechanical accuracy of ab initio simulations.
- *Change in Sec. 4.1:* While DFT relies on the self-consistent solution of the Kohn-Sham system, model III only needs a single matrix diagonalization to solve the Schrödinger equation, thus making it the fastest of all three models. Model I and II on the other hand, incorporate the Coulomb interaction through a self-consistent Hartree algorithm. Assuming a typical number of ~ 10 cycles needed for convergence the speedup should be on the order of 10^4 rather than 10^5. Most importantly, through downfolding, the matrix ~~in model III~~ of all downfolded models only covers the low-energy subspace of the electronic structure, as opposed to DFT, whose matrix accounts for low- and high energy bands.
- *Added footnote in Sec. 4.2:* ... using a similar amount of CPU hours [1]. The actual simulated times are 430 ps and 930 ps for the path integral (classical) REMD.
- *Change in Sec. 4.2:* Defining the static structure factor
- *Change in Eq. (19):*

$$S(\boldsymbol{q}) = \frac{1}{N_{\mathrm{at}}^2 \cancel{N}} \left| \sum_{l=1}^{N_{\mathrm{at}} \cancel{N}} e^{-i\boldsymbol{q}\cdot\boldsymbol{R}_l} \right|^2 \tag{8}$$

- *Change in Sec. 4.2:* The static structure factor is the frequency integrated version of the dynamic structure factor $S(\boldsymbol{q}) = \hbar \int_{-\infty}^{+\infty} S(\boldsymbol{q}, \omega) d\omega$. Furthermore, it contains both Bragg and all orders of thermal diffuse scattering contributions.
- *Change in the Conclusions:* Despite this enormous speedup and ~~an~~ complexity reduction, we demonstrated a quantitative recovery of DFT potential energy surfaces in downfolded models II and III.
- *Change in the Conclusions:* Furthermore, anharmonic force constants and non-perturbative electron-phonon couplings [96] can be incorporated into the downfolded models to expand the accuracy to even larger lattice distortions.
- *Change in the Conclusions:* Beyond potential energy surfaces, the downfolded models can also be used to study the effective electronic structure in the presence of atomic dynamics.
- *Added Data Availability Statement after the Conclusions:* The source code and data associated with this work are available on Zenodo [98].
- *Change in Appendix B:* ~~Combining Eqs. (34),~~ Inserting Eqs. (36) and (37) into Eq. (33) yields $\Delta C_{ij}^{\mathrm{III}} \ldots$
- *Change in Appendix C:* For the transformation of the electronic energies and electron-phonon couplings to the Wannier basis, we use Wannier90 [100] and the EPW code [101,~~102~~ -103].
- *Change in References: Where available, arXiv versions have been linked.*

References

[1] T Egami and S.J.L Billinge. "Underneath the Bragg Peaks". In: *Materials Today* 6 (2003), p. 57. DOI: https://doi.org/10.1016/S1369-7021(03)00635-7.

[2] Luciano T. Costa et al. "Molecular dynamics simulation of liquid trimethylphosphine". In: *The Journal of Chemical Physics* 135 (2011), p. 064506. DOI: 10.1063/1.3624408.

[3] Omar Castrejón-González et al. "Structure factor and rheology of chain molecules from molecular dynamics". In: *The Journal of Chemical Physics* 138 (2013), p. 184901. DOI: 10.1063/1.4803526.

[4] Alfred Q. R. Baron. *Introduction to High-Resolution Inelastic X-Ray Scattering*. 2020. arXiv: 1504.01098 [cond-mat.mtrl-sci].